

## Kinetic Isolation and Characterization of the Radical Rearrangement Step in Coenzyme B<sub>12</sub>-Dependent Ethanolamine Ammonia-lyase

Chen Zhu and Kurt Warncke\*

Department of Physics, Emory University, Atlanta, Georgia 30322

Received September 13, 2009; E-mail: kwarncke@physics.emory.edu

**Abstract:** The transient decay reaction kinetics of the 1,1,2,2-<sup>2</sup>H<sub>4</sub>-aminoethanol generated Co<sup>II</sup>-substrate radical pair catalytic intermediate in ethanolamine ammonia-lyase (EAL) from *Salmonella typhimurium* have been measured by using time-resolved, full-spectrum X-band continuous-wave electron paramagnetic resonance (EPR) spectroscopy in frozen aqueous solution over the temperature range of 190–207 K. The decay reaction involves sequential passage through the rearrangement step [substrate radical → product radical] and the step [product radical → diamagnetic product] that involves hydrogen atom transfer (HT) from carbon C5' of the adenosine moiety of the cofactor to the product radical C2 center. As found for the <sup>1</sup>H-substrate radical [Zhu, C.; Warncke, K. *Biophys. J.* **2008**, *95*, 5890], the decay kinetics for the <sup>2</sup>H-substrate radical over 190–207 K represent two noninteracting populations (fast decay population: normalized amplitude = 0.44 ± 0.07; observed rate constant,  $k_{\text{obs},f} = 5.3 \times 10^{-5} - 1.1 \times 10^{-3} \text{ s}^{-1}$ ; slow decay population:  $k_{\text{obs},s} = 6.1 \times 10^{-6} - 2.9 \times 10^{-4} \text{ s}^{-1}$ ). The <sup>1</sup>H/<sup>2</sup>H isotope effects (IE) for the fast and slow decay reactions are 1.4 ± 0.2 and 0.79 ± 0.11, respectively. The IE on the fast phase is uniform over the temperature interval, and the value is consistent with an α-secondary hydrogen kinetic IE, which arises from changes in the force constants of the C–H bonds in the substrate radical structure, upon passing from the substrate radical state to the rearrangement transition state. Therefore, we propose that  $k_{\text{obs},f}$  represents the rate constant for the radical rearrangement and that this step is the rate-determining step in substrate radical decay. The Arrhenius activation energy for the <sup>1</sup>H-substrate radical rearrangement (13.5 ± 0.4 kcal/mol) is consistent with values from quantum chemical calculations performed on simple models. The results show that the core, radical rearrangement reaction is culled from the catalytic cycle in the low-temperature system, thus establishing the system for detailed transient kinetic and spectroscopic analysis of protein structural and dynamic contributions to EAL catalysis.

### Introduction

The interior reactions in a multistep enzyme catalysis involve the pivotal bond-making/bond-breaking events in substrate transformation. Yet, these reactions are usually not accessible to study by informative single-step, transient kinetics measurements. The short time-scale creation of unstable intermediate states by photolysis<sup>1,2</sup> and γ-irradiation-induced reduction<sup>3,4</sup> in metalloproteins at cryogenic temperatures, followed by annealing, have been developed to study single, or short sequences of, interior reaction steps. The cryotrapping of unstable intermediates,<sup>5</sup> followed by annealing, has also been performed. We have recently reported that the cryotrapped Co<sup>II</sup>-substrate radical pair intermediate in the coenzyme B<sub>12</sub> (adenosylcobalamin)-dependent ethanolamine ammonia-lyase (EAL) [EC

4.3.1.7; cobalamin (vitamin B<sub>12</sub>)-dependent enzyme superfamily]<sup>6,7</sup> from *Salmonella typhimurium*<sup>8–10</sup> reacts to form diamagnetic products during annealing, over the temperature range of 190–217 K.<sup>11</sup> The reaction of the substrate radical is monitored by using time-resolved, full-spectrum electron paramagnetic resonance (EPR) spectroscopy.<sup>11</sup> The real-time EPR experiment is made possible by the slow time scale of the reaction in the low-temperature range ( $\tau \sim 10^3 - 10^5 \text{ s}$ ), relative to the instrument deadtime and the spectrum acquisition periods ( $\leq 6 \times 10^1 \text{ s}$ ). Here, we have examined the <sup>1</sup>H/<sup>2</sup>H hydrogen isotope effect (IE) on the low-temperature decay reaction of the Co<sup>II</sup>-substrate radical pair intermediate, with the aim of gaining insight into the rate-determining step(s) and mechanisms.

Figure 1 shows the position of the Co<sup>II</sup>-substrate radical pair state in the minimal mechanism for the catalytic cycle of EAL.<sup>8,9</sup>

- (1) Gibson, Q. H. *J. Physiol.* **1956**, *134*, 112.
- (2) Austin, R. H.; Beeson, K. W.; Eisenstein, L.; Frauenfelder, H.; Gunsalus, I. C. *Biochemistry* **1975**, *14*, 5355–5373.
- (3) Blumenfeld, L. A.; Davydov, R. M.; Magonov, S. N.; Vilu, R. O. *FEBS Lett.* **1974**, *45*, 256–258.
- (4) Blumenfeld, L. A.; Davydov, R. M.; Magonov, S. N.; Vilu, R. O. *FEBS Lett.* **1974**, *49*, 246–249.
- (5) Lukoyanov, D.; Barney, B. M.; Dean, D. R.; Seefeldt, L. C.; Hoffman, B. M. *Proc. Natl. Acad. Sci.* **2007**, *104*, 1451–1455.

- (6) Hubbard, T. J. P.; Ailey, B.; Brenner, S. E.; Murzin, A. G.; Chothia, C. *Nucleic Acids Res.* **1999**, *27*, 254–256.
- (7) Sun, L.; Warncke, K. *Proteins: Struct., Funct., Bioinf.* **2006**, *64*, 308–319.
- (8) Bandarian, V.; Reed, G. H. *Chemistry and Biochemistry of B12*; Banerjee, R., Ed.; John Wiley and Sons: New York, 1999; pp 811–833.
- (9) Toraya, T. *Chem. Rev.* **2003**, *103*, 2095–2127.
- (10) Brown, K. *Chem. Rev.* **2005**, *105*, 2075–2149.
- (11) Zhu, C.; Warncke, K. *Biophys. J.* **2008**, *95*, 5890–5900.

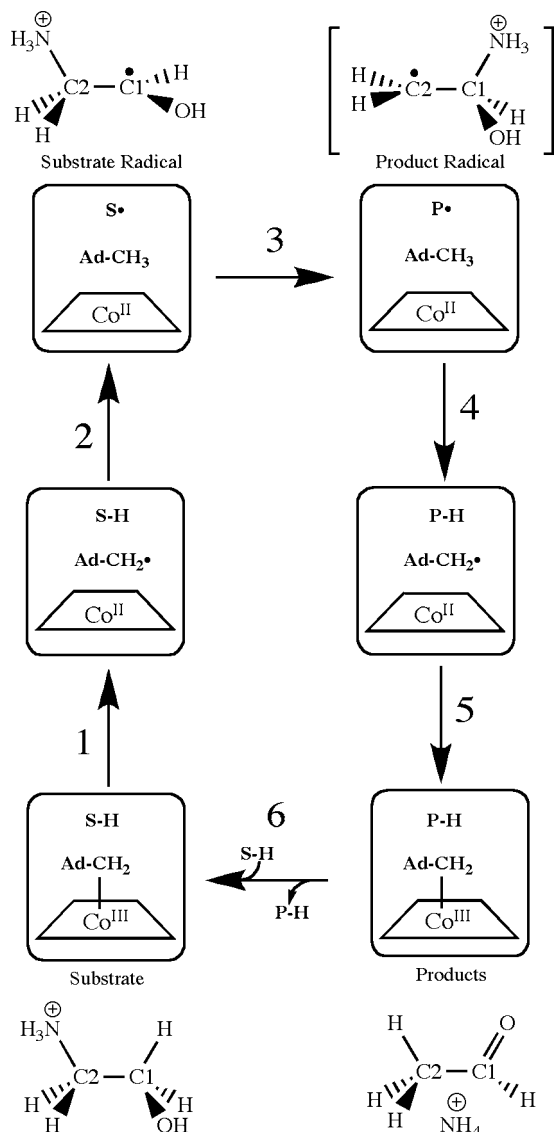


**Figure 1.** Minimal mechanism of catalysis for coenzyme B<sub>12</sub>-dependent ethanolamine ammonia-lyase (EAL) and structures of substrate, intermediates, and product.<sup>8,9</sup> The forward direction of reaction is indicated by arrows. The steps are as follows: (1) radical pair separation, (2) first hydrogen atom transfer (HT1), (3) radical rearrangement, (4) second hydrogen atom transfer (HT2), (5) radical pair recombination, and (6) product release/substrate binding. Substrate-derived species are designated S–H (bound substrate), S• (substrate radical), P• (product radical; brackets indicate proposed structure), and PH (diamagnetic products). The brackets around the product radical indicate that the structure of this intermediate is not known, although the carbinolamine is favored. The 5′-deoxyadenosyl β-axial ligand is represented as Ad-CH<sub>2</sub>• in the intact coenzyme, and as Ad-CH<sub>2</sub>• (5′-deoxyadenosyl radical) or Ad-CH<sub>3</sub>• (5′-deoxyadenosine) following cobalt–carbon bond cleavage. The cobalt ion and its formal oxidation states are depicted, but the corrin ring and the dimethylbenzimidazole α-axial ligand of the coenzyme<sup>43,44</sup> are not shown for clarity.

The Co<sup>II</sup>–substrate radical pair accumulates as the only detectable paramagnetic intermediate during room-temperature, steady-state turnover of aminoethanol by EAL.<sup>11–13</sup> As shown in Figure 1, the Co<sup>II</sup>–substrate radical pair reacts in the forward direction to form the Co<sup>II</sup>–product radical pair. The structure of the

product radical is unknown, but a carbinolamine radical is favored by analogy with the demonstrated<sup>14</sup> *gem*-diol product radical intermediate in the mechanistically similar coenzyme B<sub>12</sub>-dependent enzyme, diol dehydratase, and by theoretical studies.<sup>15,16</sup> The product radical abstracts a hydrogen atom from the C5′-methyl group of 5′-deoxyadenosine (second hydrogen atom transfer step, HT2), which produces a diamagnetic product species and reforms the 5′-deoxyadenosyl radical. Following the HT2 step, the 5′-deoxyadenosyl radical recombines with Co<sup>II</sup> to regenerate the intact coenzyme,<sup>17</sup> and products acetaldehyde and ammonia are released.<sup>18</sup>

The accumulation of the Co<sup>II</sup>–substrate radical pair as the only EPR-detectable paramagnetic intermediate during steady-state turnover on <sup>1</sup>H-aminoethanol led to the suggestion that the rearrangement step represents a significant barrier in the overall reaction.<sup>12</sup> Consistent with this observation, the <sup>1</sup>H-aminoethanol substrate <sup>14</sup>N/<sup>15</sup>N steady-state kinetic IE on *V*/*K<sub>M</sub>* (*V*, maximum velocity; *K<sub>M</sub>*, Michaelis constant) and *V*/*K<sub>M</sub>* was proposed to arise from C2–N bond cleavage in the rearrangement step.<sup>12,19</sup> However, the relatively low value of the <sup>15</sup>N-kinetic IE led to the proposal that hydrogen atom transfer was largely rate limiting in the steady-state reaction of <sup>1</sup>H-aminoethanol substrate.<sup>20</sup> The following hydrogen isotope effects suggested that hydrogen transfer, and specifically HT2, contributes to rate determination of steady-state turnover: (a) a steady-state <sup>1</sup>H/<sup>2</sup>H isotope effect on *k<sub>cat</sub>* (or equivalently, the maximum velocity, *V*) of 7.4<sup>21</sup> or 7.5,<sup>22</sup> (b) a <sup>1</sup>H/<sup>2</sup>H IE of 7.3 on transfer of hydrogen from the adenosyl C5′-methyl group to the product radical,<sup>21</sup> and (c) a <sup>1</sup>H/<sup>3</sup>H IE of 100 on hydrogen transfer from C5′ to the product radical.<sup>8,21</sup> Here, we use the substrate <sup>1</sup>H/<sup>2</sup>H IE as a method to assess the contributions of radical rearrangement and HT2 to the low-temperature decay reaction of the cryotrapped Co<sup>II</sup>–substrate radical pair.

The low-temperature decay reaction of the Co<sup>II</sup>–substrate radical pair allows a direct, transient kinetic assessment of the reaction sequence that follows the substrate radical state, in the absence of enzyme turnover. As shown previously,<sup>11</sup> the decay of the <sup>1</sup>H–substrate radical in EAL displays three regions of kinetic behavior as a function of temperature. Over the range, 190 ≤ *T* ≤ 207 K, the decay is biexponential, with constant fast phase and slow phase amplitudes and fast and slow observed rate constants (*k<sub>obs,f</sub>* and *k<sub>obs,s</sub>*) that differ by approximately 10-fold. The temperature dependence is characterized by single sets of Arrhenius prefactor (*A*) and activation energy (*E<sub>a</sub>*) parameters for the slow and fast phases, which correspond to two separate, noninterconverting populations of substrate radicals.<sup>11</sup> With increasing temperature over the range, 207 < *T* < 210 K, the normalized amplitude of the fast phase increases to unity, while the amplitude of the slow phase decreases to zero. The narrow, <4 K temperature range of this change suggests an origin in a

(12) Bender, G.; Poyner, R. R.; Reed, G. H. *Biochemistry* **2008**, *47*, 11360–11366.  
 (13) Warncke, K.; Schmidt, J. C.; Ke, S.-C. *J. Am. Chem. Soc.* **1999**, *121*, 10522–10528; *ibid.*, **2008**, *130*, 6055.

(14) Reteý, J.; Suckling, C. J.; Arigoni, D.; Babior, B. M. *J. Biol. Chem.* **1974**, *249*, 6359–6360.  
 (15) Wetmore, S. D.; Smith, D. M.; Bennet, J. T.; Radom, L. *J. Am. Chem. Soc.* **2002**, *124*, 14054–14065.  
 (16) Semialjac, M.; Schwartz, H. *J. Am. Chem. Soc.* **2002**, *124*, 8974–8983.  
 (17) Licht, S. S.; Lawrence, C. C.; Stubbe, J. *J. Am. Chem. Soc.* **1999**, *121*, 7463–7468.  
 (18) Bradbeer, C. *J. Biol. Chem.* **1965**, *240*, 4669.  
 (19) Poyner, R. R.; Anderson, M. A.; Bandarian, V.; Clelland, W. W.; Reed, G. H. *J. Am. Chem. Soc.* **2006**, *128*, 7120–7121.  
 (20) Frey, P. A. *Comprehensive Natural Products II: Chemistry and Biology*; Mander, L., Lui, H.-W., Eds.; Elsevier: Oxford, 2010; Vol. 7, pp 501–546.  
 (21) Weisblat, D. A.; Babior, B. M. *J. Biol. Chem.* **1971**, *246*, 6064–6071.  
 (22) Bandarian, V.; Reed, G. H. *Biochemistry* **2000**, *39*, 12069–12075.

protein dynamical transition.<sup>11</sup> At  $T \geq 210$  K, the decay is monoexponential, with  $A$  and  $E_a$  parameters that match those for the fast phase decay component at 190–207 K. To address the molecular mechanisms of the decay and the emergence of the slow phase at  $T < 207$  K, the step(s) represented by  $k_{\text{obs},f}$  and  $k_{\text{obs},s}$  must be identified.

We have cryotrapped the  $\text{Co}^{\text{II}}$ –substrate radical pair formed during turnover of EAL on 1,1,2,2- $^2\text{H}_4$ -aminoethanol and measured the kinetics of the fast and slow decay populations after temperature step to 190–207 K. Turnover on the  $^2\text{H}_4$ -aminoethanol incorporates  $^2\text{H}$  into all catalytically exchangeable hydrogen sites after two enzyme turnovers.<sup>22</sup> Prior to cryotrapping, the  $^2\text{H}$ -aminoethanol substrate samples execute  $>20$  turnovers. Therefore, in the starting state for the low-temperature decay, the C1-methylene, C2-methylene, and C5'-methyl hydrogen sites are all  $^2\text{H}$ -labeled in the  $^2\text{H}$ –substrate radical state, and HT2 proceeds by deuterium transfer. The first-order decay rate constants for the  $^2\text{H}$ –substrate radical are compared with the previously measured<sup>11</sup> first-order decay rate constants obtained for the natural abundance,  $^1\text{H}$ –substrate radical over the temperature range of 190–207 K. If HT2 participates in rate limitation, then a primary kinetic IE that is significantly greater than unity is expected. We observe modest, constant IEs for each kinetic phase from 190 to 207 K, which are not consistent with rate determination by HT2, and conclude that  $k_{\text{obs},f}$  represents the rate constant for radical rearrangement.

## Materials and Methods

**Enzyme Preparation.** Enzyme was purified from the *Escherichia coli* overexpression strain incorporating the cloned *S. typhimurium* EAL coding sequence<sup>23</sup> essentially as described,<sup>24</sup> with the exceptions that the enzyme was dialyzed against buffer containing 100 mM HEPES (pH 7.5), 10 mM potassium chloride, 5 mM dithiothreitol, and 10% glycerol,<sup>25</sup> and neither Triton X-100 nor urea was used during the purification. Enzyme activity was determined as described<sup>26</sup> by using the coupled assay with alcohol dehydrogenase/NADH. The specific activity of the purified enzyme with aminoethanol as substrate was 20–30  $\mu\text{mol}/\text{min}/\text{mg}$ .

**Sample Preparation.** Adenosylcobalamin (Sigma Chemical Co.), 1,1,2,2- $^2\text{H}_4$  aminoethanol (Cambridge Isotope Laboratories, Inc.), and natural abundance aminoethanol (Aldrich Chemical Co.) were purchased from commercial sources. The reactions were performed in air-saturated buffer containing 10 mM potassium phosphate (pH 7.5). The kinetic parameters were identical in anaerobic samples. All manipulations were carried out on ice under dim red safe-lighting. The final concentration of enzyme was 10–15 mg/mL, which is equivalent to 20–30  $\mu\text{M}$  for a holoenzyme molecular mass of 500 000 g/mol<sup>24</sup> and an active site concentration of 120–180  $\mu\text{M}$ , based on an active site/holoenzyme stoichiometry of 6:1.<sup>27,28</sup> Adenosylcobalamin was added to 240–360  $\mu\text{M}$  (2-fold excess over active sites).

The  $\text{Co}^{\text{II}}$ –substrate radical pair samples were prepared by using a procedure for fast cryotrapping of steady-state intermediate states in EAL.<sup>13</sup> Briefly, following manual mixing of the holoenzyme solution with the substrate solution (both prepared in 10 mM potassium phosphate buffer, pH = 7.5), the sample was loaded into a 4 mm outer diameter EPR tube, and the tube was plunged into

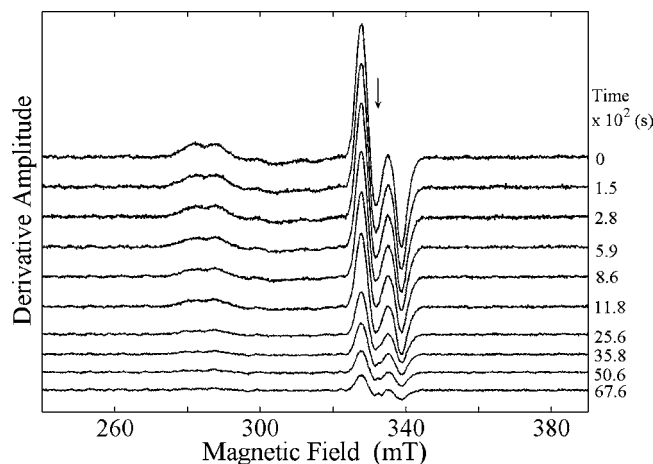


**Figure 2.** Dependence of the EPR spectrum of the  $^2\text{H}_4$ -aminoethanol-generated  $\text{Co}^{\text{II}}$ –substrate radical pair state in EAL on time at  $T = 207$  K after temperature-step reaction initiation. The free electron resonance position at  $g = 2.0$  is shown by the arrow. *Experimental Conditions:* microwave frequency, 9.3434 GHz; microwave power, 20.25 mW; magnetic field modulation, 1.0 mT; modulation frequency, 100 kHz; scan rate, 6.52 mT/s; time constant, 2.56 ms.

liquid-nitrogen-chilled isopentane ( $T \approx 150$  K) to trap the  $\text{Co}^{\text{II}}$ –substrate radical pair state. The total elapsed time from mixing to isopentane immersion was 15 s. The  $\text{Co}^{\text{II}}$ –substrate radical pair to active site ratio is 0.2.<sup>13,14</sup>

**Continuous-Wave EPR Spectroscopy.** EPR spectra were obtained by using a Bruker E500 ElexSys EPR spectrometer equipped with a Bruker ER4123 SHQE cavity. Temperature was controlled with a Bruker ER4131VT liquid nitrogen/gas flow cryostat system, with ER4121VT-1011 evaporator/transfer line, ER4121VT-1013 heater/thermocouple, and 26 L liquid nitrogen reservoir. For the decay experiments, this temperature control system allowed rapid temperature step changes, relative to the more slowly responding Oxford ESR900 cryostat, and run times of up to  $2\text{--}3 \times 10^4$  s, depending upon flow rate. Measurements were performed under dim light and with the EPR tubes inserted into the EPR resonator, which shielded the samples from direct exposure to light. Under these conditions with frozen samples, sample degradation owing to coenzyme photolysis is negligible.

**Time-Resolved EPR Measurements.** EPR samples were held at a staging temperature of 160 or 180 K in the ER4131VT cryostat system in the Bruker E500 spectrometer, and the microwave bridge was tuned. Temperature steps from 160 or 180 K to the decay measurement temperatures of 190, 193, 197, 200, 203, or 207 K were initiated by changing the ER4131VT temperature set point. Once the sample temperature stabilized at the set point, the preset autotune/autoscan mode of the spectrometer was triggered, and the sample was autotuned at the high-temperature set point, followed immediately by continuous spectrum acquisition. The time from initiation of the temperature step to the start of acquisition of the first spectrum was  $3.0\text{--}6.0 \times 10^1$  s. The zero time of the decay was marked at the first collected EPR spectrum. The EPR spectra were acquired with a 24 s sweep time (2.56 ms time constant). The reported temperatures represent the temperature at the sample, which was determined prior to each decay run by using an Oxford Instruments ITC503 temperature controller with a calibrated model 19180 4-wire RTD probe, which has  $\pm 0.3$  K accuracy over the decay measurement temperature range. For measurements over the temperature range, 190–207 K, the ER4131VT cryostat/controller system provided a temperature stability of  $\pm 0.5$  K over the length of the EPR sample cavity, as measured by using a thermocouple probe that was translated along the EPR tube axis to achieve different heights within a solution sample. The temperature was therefore stable to  $\pm 0.5$  K during each run.

(23) Faust, L. P.; Connor, J. A.; Roof, D. M.; Hoch, J. A.; Babior, B. M. *J. Biol. Chem.* **1990**, *265*, 12462–12466.

(24) Faust, L. P.; Babior, B. M. *Arch. Biochem. Biophys.* **1992**, *294*, 50–54.

(25) Harkins, T.; Grissom, C. B. *J. Am. Chem. Soc.* **1995**, *117*, 566–567.

(26) Kaplan, B. H.; Stadtman, E. R. *J. Biol. Chem.* **1968**, *243*, 1787–1793.

(27) Hollaway, M. R.; Johnson, A. W.; Lappert, M. F.; Wallis, O. C. *Eur. J. Biochem.* **1980**, *111*, 177–188.

(28) Bandarian, V.; Reed, G. H. *Biochemistry* **1999**, *38*, 12394–12402.

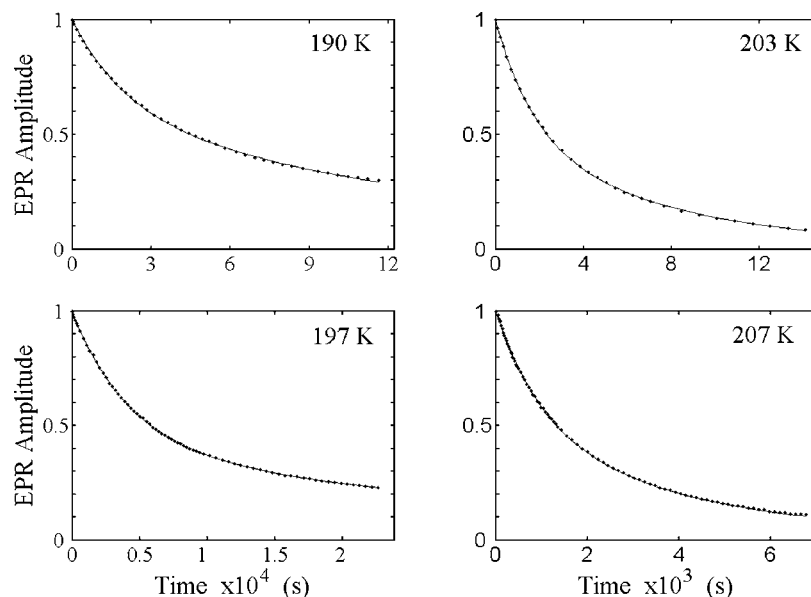


**Figure 3.** Decay of the amplitude of the  $^2\text{H}_4$ -aminoethanol-generated substrate radical as a function of time at selected temperatures from 190–207 K and overlaid best-fit biexponential function (line). The EPR experimental conditions are as described in the legend to Figure 2. The simulation parameters are presented in Table 1.

**Kinetic Analysis.** EPR spectra acquired continuously during the decay were used directly in the kinetic analysis or were averaged in blocks of 2–20 spectra to increase the signal-to-noise ratio (SNR), and the acquisition time was calculated as the average time for the block. For each EPR spectrum, the amplitude of  $\text{Co}^{\text{II}}$  was obtained from the difference between the baseline and the peak feature at  $g \approx 2.3$ , and the substrate radical amplitude was obtained from the difference between peak and trough amplitudes of the derivative feature around  $g \approx 2.0$ . All data processing programs were written in Matlab (Mathworks, Natick, MA). The observed decays were fitted to biexponential (eq 1,  $N = 2$ ) functions by using the following expression

$$\frac{A(t)}{A(0)} = \sum_{i=1}^N A_i e^{-k_i t} \quad (1)$$

where  $A(t)/A(0)$  is the normalized total amplitude;  $A_i$  is the normalized component amplitude ( $\sum_{i=1}^N A_i = 1$  at  $t = 0$ ); and  $k_i$  is the first-order rate constant. The fitting of the data was performed by using Origin (OriginLab, Natick, MA).

**Temperature Dependence of the First-Order Rate Constant.** The temperature dependence of the first-order rate constant,  $k$ , is given by the Arrhenius expression, as follows<sup>29</sup>

$$k(T) = A e^{-E_a/RT} \quad (2)$$

where  $E_a$  is the activation energy;  $R$  is the gas constant; and  $A$  is a prefactor that represents the value of  $k$  as  $T \rightarrow \infty$ . In a plot of  $\ln k$  versus  $T^{-1}$  (Arrhenius plot), the intercept of the linear relation is given by  $\ln A$ , and the slope is given by  $-E_a/R$ .

## Results

**$^2\text{H}_4$ -Aminoethanol-Generated  $\text{Co}^{\text{II}}$ -Substrate Radical Pair EPR Spectrum.** Figure 2 shows the zero-time EPR spectrum of the  $^2\text{H}_4$ -aminoethanol-derived  $\text{Co}^{\text{II}}$ -substrate radical pair at the representative annealing temperature of 207 K. The  $\text{Co}^{\text{II}}$  EPR signal intensity is most prominent in the region around 285 mT, which is near to the  $g_{\perp} = 2.26$  value in the EPR

spectrum of isolated cob(II)alamin.<sup>30</sup> The  $\text{Co}^{\text{II}}$  features in the radical pair spectrum are broadened, relative to isolated cob(I)-alamin, by the interaction with the unpaired electron localized on C1 of the substrate radical.<sup>31</sup> The substrate radical line shape extends from approximately 325 to 345 mT. The partially resolved doublet splitting and inhomogeneous broadening is caused by the interaction with the unpaired electron spin on  $\text{Co}^{\text{II}}$ .<sup>13,31</sup> All of the features of the  $\text{Co}^{\text{II}}$ -substrate radical pair spectrum can be accounted for by EPR simulations.<sup>32,33</sup>

**Time-Resolved Measurements of EPR Spectra During the  $^2\text{H}_4$ -Aminoethanol Substrate Radical Decay Reaction.** Figure 2 shows a stack plot of a selection of 11 of the 300 total EPR spectra that were collected during the course of a representative decay of the  $^2\text{H}_4$ -aminoethanol-generated  $\text{Co}^{\text{II}}$ -substrate radical pair at 207 K. Decay data were collected for temperatures of 190, 193, 197, 200, 203, and 207 K. The  $\text{Co}^{\text{II}}$  and substrate radical EPR signals decay in synchrony, and no EPR signals from paramagnetic species, other than the  $\text{Co}^{\text{II}}$ -substrate radical pair, were detected at a signal-to-noise ratio of  $10^2$  for the peak-to-trough amplitude of the substrate radical, as found for the decay of the  $^1\text{H}_4$ -aminoethanol-generated  $\text{Co}^{\text{II}}$ -substrate radical pair.<sup>11</sup>

**Time and Temperature Dependence of the  $^2\text{H}_4$ -Aminoethanol Substrate Radical Decay Reaction.** Figure 3 shows representative decays of the substrate radical EPR signal as a function of time at temperatures of 190, 197, 203, and 207 K. The theoretical curves in Figure 3 represent fits of the data to a biexponential function (eq 1,  $N = 2$ ). The biexponential function provides an excellent fit to the decay at all of the temperatures examined from 190 to 207 K. The rate constants,  $k_{\text{obs,f}}$  and  $k_{\text{obs,s}}$ , and normalized amplitude coefficients,  $A_{\text{obs,f}}$  and  $A_{\text{obs,s}}$ , for the fast and slow phases of the biexponential fitting functions for

(29) Moore, J. W.; Pearson, R. G. *Kinetics and Mechanism*; Wiley and Sons: New York, 1981.

(30) Pilbrow, J. R. *B12*; Dolphin, D., Ed.; Wiley: New York, 1982; Vol. 1, pp 431–462.

(31) Boas, J. F.; Hicks, P. R.; Pilbrow, J. R.; Smith, T. D. *J. Chem. Soc., Faraday II* **1978**, *74*, 417–431.

(32) Canfield, J. M.; Warncke, K. *J. Phys. Chem. B* **2005**, *109*, 3053–3064.

(33) Ke, S.-C. *Biochim. Biophys. Acta* **2003**, *1620*, 267–272.

**Table 1.** Observed First-Order Rate Constants and Normalized Amplitude Parameters for Fits of the Biexponential Function to the Decay Kinetics of the  $^2\text{H}$ -Substrate Radical State and  $^1\text{H}/^2\text{H}$  Hydrogen Isotope Effects (IE) at Different Temperatures<sup>a</sup>

<i>T</i> (K)	$k_{\text{obs},f}$ (s <sup>-1</sup> )	$A_{\text{obs},f}^b$	$k_{\text{obs},s}$ (s <sup>-1</sup> )	$A_{\text{obs},s}^c$	$R^d$	IE <sub>f</sub>	IE <sub>s</sub>
207	$1.1 \pm 0.3 \times 10^{-3}$	$0.53 \pm 0.05$	$2.9 \pm 0.6 \times 10^{-4}$	$0.47 \pm 0.05$	0.9997	$1.4 \pm 0.2$	$1.00 \pm 0.22$
203	$5.7 \pm 0.8 \times 10^{-4}$	$0.52 \pm 0.06$	$1.1 \pm 0.1 \times 10^{-4}$	$0.48 \pm 0.06$	0.9999	$1.5 \pm 0.1$	$0.73 \pm 0.05$
200	$4.4 \pm 1.2 \times 10^{-4}$	$0.41 \pm 0.09$	$7.7 \pm 1.8 \times 10^{-5}$	$0.59 \pm 0.09$	0.9997	$1.3 \pm 0.1$	$0.61 \pm 0.04$
197	$2.6 \pm 0.2 \times 10^{-4}$	$0.44 \pm 0.11$	$3.6 \pm 0.8 \times 10^{-5}$	$0.56 \pm 0.11$	0.9998	$1.4 \pm 0.1$	$0.67 \pm 0.07$
193	$1.2 \pm 0.2 \times 10^{-4}$	$0.37 \pm 0.02$	$1.5 \pm 0.3 \times 10^{-5}$	$0.63 \pm 0.02$	0.9995	$1.2 \pm 0.3$	$0.87 \pm 0.08$
190	$5.3 \pm 0.5 \times 10^{-5}$	$0.38 \pm 0.02$	$6.1 \pm 0.1 \times 10^{-6}$	$0.62 \pm 0.02$	0.9995	$1.4 \pm 0.1$	$0.85 \pm 0.03$

<sup>a</sup> The standard deviations for the  $k_{\text{obs}}$  and  $A_{\text{obs}}$  parameters represent at least three separate determinations at each temperature. The  $^1\text{H}$ -substrate radical  $k_{\text{obs}}$  values used to calculate IE<sub>f</sub> and IE<sub>s</sub> were determined previously.<sup>11</sup> <sup>b</sup> The relative fitted amplitude for the fast phase, normalized to the sum,  $A_{\text{obs},f} + A_{\text{obs},s}$ . <sup>c</sup> The relative fitted amplitude for the slow phase, normalized to the sum,  $A_{\text{obs},f} + A_{\text{obs},s}$ . <sup>d</sup>  $R$  is Pearson's correlation coefficient.

each temperature are presented in Table 1. Table 1 shows that  $A_{\text{obs},f}$  and  $A_{\text{obs},s}$  remain comparable as the rate constants increase with increasing temperature, with mean values and standard deviations as follows:  $A_{\text{obs},f} = 0.46 \pm 0.10$  and  $A_{\text{obs},s} = 0.54 \pm 0.10$ . The kinetic fitting results are consistent with complete decay at all temperatures. The complete decay of the substrate radical EPR amplitude indicates that at least one step in the recombination process is irreversible.

## Discussion

**Isotope Effect on the Fast Phase of the Substrate Radical Decay Reaction.** Table 1 shows the values of the  $^1\text{H}/^2\text{H}$  IE for the rate constants,  $k_{\text{obs},s}$  and  $k_{\text{obs},f}$ , at each temperature from 190 to 207 K. The IE values were calculated by using the ratio of the  $k_{\text{obs}}$  value for the  $^1\text{H}$ -substrate radical ( $k_{\text{obs},s,\text{H}}$ ,  $k_{\text{obs},f,\text{H}}$ ) reported previously<sup>11</sup> and the corresponding  $k_{\text{obs}}$  values for the  $^2\text{H}$ -substrate radical ( $k_{\text{obs},s,\text{D}}$ ,  $k_{\text{obs},f,\text{D}}$ ), which are presented in Table 1. The mean IE for  $k_{\text{obs},f}$  over the temperature range of 190–207 K is  $1.4 \pm 0.2$ . The standard deviation of 0.2 represents the error propagation of the standard deviations of the measurements at each temperature. The value of 1.4 is lower than the steady-state  $^1\text{H}/^2\text{H}$  isotope effects on  $k_{\text{cat}}$  (or equivalently, the maximum velocity,  $V$ ) of  $7.4^{21}$  or  $7.5^{22}$  lower than the  $^1\text{H}/^2\text{H}$  IE of 7.3 on transfer of hydrogen from the C5'-methyl group of the cofactor to the product radical,<sup>21</sup> and also lower than the  $^1\text{H}/^2\text{H}$  IE of 17 on hydrogen transfer from C5' to product radical, which is predicted from the  $^1\text{H}/^3\text{H}$  IE,<sup>21</sup> by using classical theory.<sup>8</sup> These results show that the  $^1\text{H}/^2\text{H}$  IE on the reaction of the substrate radical decreases with decreasing temperature and, therefore, that the contribution of the HT2 step to determination of the rate of the substrate radical decay reaction decreases with decreasing temperature.

Table 1 shows that the IE of  $1.4 \pm 0.2$  is maintained over the temperature range of 190–207 K. This indicates that the decrease in the rate-determining contribution of the HT2 step occurs at  $T > 207$  K and suggests that the residual, constant IE of 1.4 over the temperature range of 190–207 K arises from a different source. A minimal kinetic model for the irreversible substrate radical decay through the rearrangement and HT2 steps is presented in Figure 4. The following general expression for  $k_{\text{obs},f}$  is derived from this model<sup>29</sup>

$$k_{\text{obs},f} = \frac{k_{\text{SP}}k_{\text{HT}}}{k_{\text{PS}} + k_{\text{HT}}} \quad (3)$$

The absence of a contribution of  $k_{\text{HT}}$  to  $k_{\text{obs},f}$  is consistent with eq 3, if the condition,  $k_{\text{PS}} \ll k_{\text{HT}}$ , holds. In this case,  $k_{\text{obs},f} = k_{\text{SP}}$ , and the hydrogen IE on  $k_{\text{obs},f}$  corresponds to  $(k_{\text{SP},\text{H}})/(k_{\text{SP},\text{D}})$ . The IE of 1.4 on  $k_{\text{obs},f}$  suggests an  $\alpha$ -secondary kinetic IE, which arises from changes in the force constants of the C–H bonds in the substrate radical structure, upon passing from the substrate

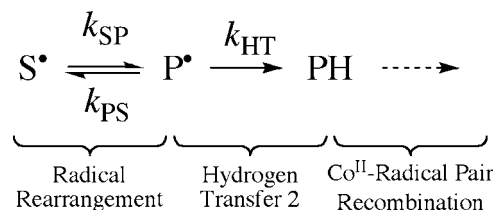


**Figure 4.** Simple kinetic model for the decay reaction of the cryotrapped substrate radical at 190–207 K. The states are designated as follows: S\*, substrate radical; P\*, product radical; PH, diamagnetic product.

radical state to the rearrangement transition state.<sup>34,35</sup> The  $\alpha$ -secondary kinetic IE for the change of hybridization of carbon from  $\text{sp}^3$  to  $\text{sp}^2$  is typically 1.1–1.2, and the theoretical maximum value has been calculated to be 1.4.<sup>36</sup> Therefore, we propose that the fast phase of decay of the substrate radical is rate-determined by the radical rearrangement step for both  $^1\text{H}$ - and  $^2\text{H}$ -substrate and that  $k_{\text{obs},f}$  represents the first-order rate constant for this step.

**Isotope Effect on the Slow Phase of the Substrate Radical Decay Reaction.** The mean IE for  $k_{\text{obs},s}$  over the temperature range of 190–207 K is  $0.79 \pm 0.11$ . This inverse IE on  $k_{\text{obs},s}$  indicates that a normal primary kinetic IE from HT2 also does not contribute significantly to rate determination of the slow phase of the substrate radical decay reaction. The origin of the inverse IE on  $k_{\text{obs},s}$  is not clear, at present. The differences in the values of  $k_{\text{obs},s}$  and  $k_{\text{obs},f}$ , which have been attributed to a difference in protein structure, dynamics, or both,<sup>11</sup> and the different IE on  $k_{\text{obs},s}$  and  $k_{\text{obs},f}$  indicate that different microscopic events are rate determining for the fast and slow decays. For example, if the protein influence shifts the transition state for rearrangement to a later position on the N-migration coordinate, then the development of significant  $\text{sp}^2$ -hybridization at both C1 and C2 in an associative, cyclopropyl transition state,<sup>37</sup> or in a dissociative allyloxy transition state,<sup>38,39</sup> may lead to an inverse  $\alpha$ -secondary kinetic isotope effect. Additional substrate hydrogen IE studies, performed with substrate labeled specifically at C1 or C2 and with rapid trapping to minimize label scrambling among the substrate and C5' C–H sites, may identify the origin of the inverse IE.

**Temperature Dependence of the Observed Fast-Phase Rate Constants.** Figure 5 shows plots of the natural logarithms of  $k_{\text{obs},f}$  as a function of inverse absolute temperature for the

(34) Cook, P. F. *Enzyme mechanisms from isotope effects*; CRC Press: Boca Raton, 1991.

(35) Cleland, W. W. *J. Biol. Chem.* **2003**, *278*, 51975–51984.

(36) Anslyn, E. V.; Dougherty, D. A. *Modern Physical Organic Chemistry*; University Science Books: Sausalito, California, 2006.

(37) Golding, B. T. *B12*; Dolphin, D., Ed.; Wiley: New York, 1982; Vol. 1, Chapter 15.

(38) Foster, T.; West, P. R. *Can. J. Chem.* **1974**, *52*, 3589–3598.

(39) Foster, T.; West, P. R. *Can. J. Chem.* **1974**, *52*, 4009–4017.

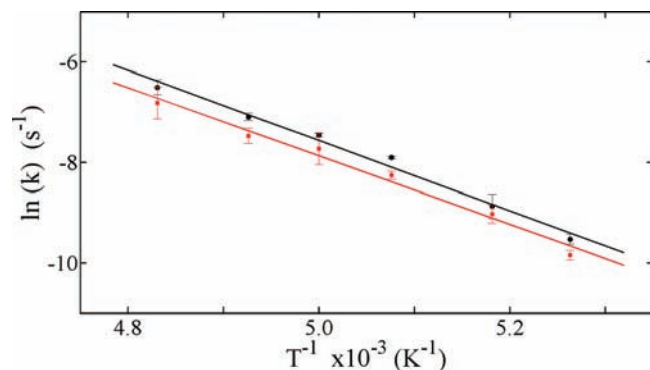


**Figure 5.** Arrhenius plots of the observed first-order rate constants for the fast phase of decay of the  $\text{Co}^{\text{II}}$ -substrate radical pair states, which were generated by using natural abundance ( $^1\text{H}$ -aminoethanol) substrate. Data from Table 1 for the  $^1\text{H}$ -substrate radical  $k_{\text{obs},f}$  (black solid circles) and for the  $^2\text{H}$ -substrate radical  $k_{\text{obs},f}$  (red solid squares) are shown. The linear fits of the Arrhenius expression for the  $^1\text{H}$ -substrate radical (black lines) and for the  $^2\text{H}$ -substrate radical (red lines) are overlaid on the data. The  $A$  and  $E_a$  values derived from the fitting parameters are collected in Table 2.

**Table 2.** Arrhenius Parameters for the Fast Phase of the  $^2\text{H}$ - and  $^1\text{H}$ -Substrate Radical Decay Kinetics for the Temperature Range 190–207 K

substrate	$\log[A \text{ (s}^{-1}\text{)}]$	$E_a \text{ (kcal mol}^{-1}\text{)}$	$R^{2a}$
$^2\text{H}$ -aminoethanol	$11.4 \pm 0.9$	$13.5 \pm 0.4$	0.9920
$^1\text{H}$ -aminoethanol	$11.9 \pm 0.9$	$13.9 \pm 0.4$	0.9935

<sup>a</sup>  $R$  is Pearson's correlation coefficient.

reaction of the  $^1\text{H}$ -substrate and  $^2\text{H}$ -substrate radicals and linear fits of eq 3 to the two sets of data points. As concluded in the previous section, the  $k_{\text{obs},f}$  values represent the rearrangement reaction step. Therefore, application of the Arrhenius analysis of the first-order rate constant is appropriate. Table 2 shows that the logarithms of the Arrhenius prefactors,  $A_{f,H}$  and  $A_{f,D}$ , and activation energies,  $E_{af,H}$  and  $E_{af,D}$ , for the  $^1\text{H}$ - and  $^2\text{H}$ -substrate radical reactions are pairwise the same, to within one standard deviation. The absence of a significant hydrogen IE on the Arrhenius parameters agrees with the absence of a large primary hydrogen kinetic IE.

The experimental fast-phase activation energies of  $13.5 \pm 0.4$  kcal/mol ( $^1\text{H}$ ) and  $13.9 \pm 0.4$  kcal/mol ( $^2\text{H}$ ) (Table 2) are the first directly measured  $E_a$  values for a radical rearrangement step in a coenzyme  $\text{B}_{12}$ -dependent enzyme. The values of the Arrhenius prefactors of  $2.5 \times 10^{11}$  to  $7.9 \times 10^{11} \text{ s}^{-1}$  differ by

less than 17-fold from  $(k_{\text{B}}T)/(h) = 4.2 \times 10^{12} \text{ s}^{-1}$  for  $T = 200$  K, which indicates that the rate-determining events in rearrangement are accompanied by relatively small activation entropy contributions ( $<5.6$  cal/mol/K). Therefore, comparisons of the experimental  $E_a$  values with values obtained by high-level quantum chemical calculations on restricted-atom models are appropriate. Values of 16 kcal/mol<sup>15</sup> and 12–15 kcal/mol<sup>40</sup> were obtained from ab initio calculations for the rearrangement reaction in EAL. The calculations were based on models that included the aminoethanol substrate and different associated molecules, which represented putative active site amino acid side chains.<sup>15,40</sup> The auxiliary molecules assisted the nitrogen migration through the formation of hydrogen bonds with the ammonium group (“push” catalyst)<sup>41</sup> or the substrate hydroxyl oxygen (“pull” catalyst).<sup>41</sup> The calculations suggested that the lowest-energy rearrangement pathway proceeds by an associative mechanism.<sup>15,40</sup> Active site arginine and glutamate side chains have been identified as substrate hydrogen bonding partners in the structural proteomics model for the EutB protein of EAL.<sup>7,42</sup> The protein structure and experimental  $E_a$  values are thus consistent with the proposed “retro push–pull” hydrogen bonding mechanism<sup>41</sup> of radical rearrangement catalysis in EAL.<sup>15,41</sup>

**Comparison of Fast-Phase Substrate Radical Decay at 190–207 K and Steady-State Turnover at 298 K.** The accumulation of the  $\text{Co}^{\text{II}}$ -aminoethanol substrate radical pair as the only paramagnetic intermediate under steady-state turnover conditions<sup>12</sup> and the substrate  $^{14}\text{N}/^{15}\text{N}$  IE on  $V/K_{\text{M}}$  and  $V^{12,19}$  indicate that the rearrangement step presents a significant barrier to the overall steady-state reaction sequence, for the  $^1\text{H}$ -aminoethanol substrate,<sup>12</sup> but the relatively small value of the  $^{15}\text{N}$ -kinetic IE (0.17%)<sup>19</sup> led to the proposal that hydrogen transfer is largely rate limiting for the steady-state reaction at room temperature.<sup>20</sup> In contrast, the results and interpretation, presented here, establish that the radical rearrangement is the dominant rate-determining step in the decay reaction of the cryotrapped substrate radical at 190–207 K. The low-temperature results lead to the prediction that the rate constant for the HT2 step is temperature dependent ( $k_{\text{HT}}$  decreases with decreasing temperature) because the rate constant for radical rearrangement is relatively temperature independent (small activation entropy). The relation of the mechanism for the low- and high-temperature regimes, in the context of the model presented in Figure 4, will be further addressed, by studying the kinetics of the  $^1\text{H}$ - and  $^2\text{H}$ -substrate radical decay reactions over a more extensive range of temperatures.

**Acknowledgment.** The project described was supported by Grant Number R01DK054514 from the National Institute of Diabetes and Digestive and Kidney Diseases. The Bruker E500 EPR spectrometer was funded by NIH NCRR Grant RR17767 and by Emory University.

JA907769G

- (40) Semialjac, M.; Schwartz, H. *J. Org. Chem.* **2003**, *68*, 6967–6983.  
 (41) Smith, D. M.; Golding, B. T.; Radom, L. *J. Am. Chem. Soc.* **2001**, *123*, 1664–1675.  
 (42) Sun, L.; Groover, O. A.; Canfield, J. M.; Warncke, K. *Biochemistry* **2008**, *47*, 5523–5535.  
 (43) Ke, S.-C.; Torrent, M.; Museav, D. G.; Morokuma, K.; Warncke, K. *Biochemistry* **1999**, *38*, 12681–12689.  
 (44) Abend, A.; Bandarian, V.; Nitsche, R.; Stupperich, E.; Reley, J.; Reed, G. H. *Arch. Biochem. Biophys.* **1999**, *370*, 138–141.